Beam-Target helicity asymmetry in charged pion photo-production from polarized neutrons in solid HD using the CLAS at Jefferson Lab

T. Kageya[1], D. Ho[2], P. Peng[3], F. Klein[4], A.M. Sandorfi[1], and R. Schumacher[2]

[1] *Thomas Jefferson National Accelerator Facility, Newport News, VA 23606, USA*
[2] *Carnegie Mellon University, Pittsburgh, PA 15213, USA*
[3] *University of Virginia, Charlottesville, VA 22903 USA and*
[4] *George Washington University, Washington, DC 20052, USA*

(for the CLAS Collaboration)

(Dated: February 2, 2017)

Single charged-pion photoproduction from circularly polarized photons and longitudinally-polarized deuterons has been measured in the CLAS detector at Jefferson Lab. Preliminary E asymmetries for the exclusive reaction, $\gamma + \mathrm{n(p)} \to \pi^- + \mathrm{p(p)}$, have been extracted with three very different methods and are in excellent agreement. These data are expected to provide significant new constraints on photoproduction multipoles from the neutron for which data are sparse.

I. INTRODUCTION

Recent Lattice QCD calculations have supported the long standing quark model expectation of many more excited states of the nucleon than have been experimentally observed. These missing states are expected to be broad and overlapping and require detailed partial wave analyses (PWA) to disentangle. Measurements of many polarization observables are required to constrain PWA and data for the neutron are sparse. The E06-101 (g14) experiment was performed in Hall B of the Thomas Jefferson National Accelerator Facility (JLab), during the period from December 2011 to May 2012. Data included in the present analysis were taken with circularly polarized photon beams of energy between 0.85 to 2.4 GeV, yielding 4.1 x 10^9 trigger events.

Frozen-spin hydrogen-deuteride (HD) targets [1, 2] were used to provide longitudinally polarized quasi-free neutrons. The HD In-Beam Cryostat (IBC) [2] operated as a dilution refrigerator and maintained targets at 50 mK in an 0.9 T superconducting solenoid. The target polarizations were calibrated in a separate production dewar and monitored by NMR in the IBC. Average deuteron polarizations were about 26% during experiments and the relaxation time for the deuteron polarization was measured to be more than a year for the run periods in this analysis.

The E asymmetry is defined as in Eq. (1) and obtained from P_γ (photon beam polariztion), P_D (D polarization in HD target), σ_p and σ_a which are yields whose photon and D spins are parallel and anti-parallel, respectively.

$$E = \frac{1}{P_\gamma \times P_D} \times \frac{\sigma_a - \sigma_p}{\sigma_a + \sigma_p}. \quad (1)$$

Three different analysis techniques have been applied to the data to extract the E asymmetries: (A) conventional background suppression via sequential requirements (cuts) and empty-cell subtraction, and advanced statistical methods that employed (B) kinematic fitting and (C) a Boosted Decision Tree (BDT) algorithm. These are compared and combined in the subsequent sections.

II. DATA REDUCTION

Circularly polarized gamma-ray beams were produced by the bremsstrahlung of electrons that were longitudinally polarized (typically to 85%). Photon energies were defined by the detection of the post-bremsstrahlung electrons in a tagging spectrometer. This analysis focused on the $\pi^- p$ final state, with particles detected in the CEBAF Large Acceptance Spectrometer (CLAS) [3]. Multiple reaction channels were used to calibrate both the tagging spectrometer and the CLAS detector.

In each of the three analysis methods, a π^- and a proton were identified using the correlation between velocity, calculated from time of flight (TOF), and particle momentum, as measured by drift chambers within the CLAS torus magnetic field. The selection was restricted to events in which only one π^- and one proton were detected. Corrections were made for the energy losses of the charged particles as they emerged from the target material and traversed the CLAS detector.

To select quasi-free neutrons, each analysis also restricted events to those with a missing momentum for an undetected proton from the $\gamma + \mathrm{n(p)} \to \pi^- p\ \mathrm{(p)}$ reaction of ≤ 0.1 GeV. (Tighter restrictions had no significant effect on the extracted asymmetries.) More cuts were applied to the three different methods described as below.

Tracking of the charged particles in the CLAS drift chambers allowed the reconstruction of the reaction vertex. The results for full and empty target cells are shown in Figure 1. The arrows indicate the regions included in the different analyses.

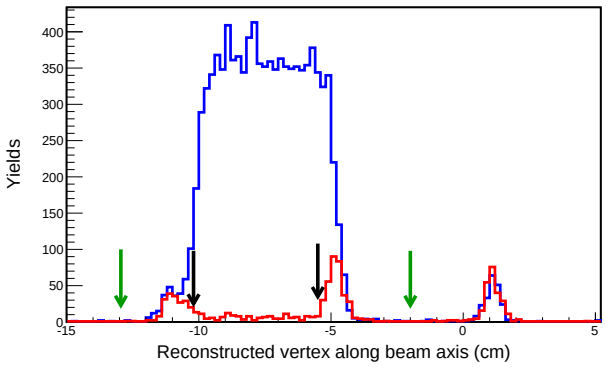

FIG. 1. The reaction vertex for a sample of data, reconstructed along the beam axis with the horizontal scale in cm, is shown for full (blue) and empty (red) target cells, normalized to the same photon flux. (The peak centered near +1 cm is generated by a foil within the cryostat and is independent of the target.) The arrows delimit the regions included in the (A) Background subtraction (green arrows), and (B) and (C) advanced statistical analyses (black arrows).

A. Background subtraction

In a conventional *Background subtraction* a sequence of cuts was applied to isolate the final state. Since in the quasi-free limit the desired reaction is 2-body, events in which the azimuthal angle difference between the proton and the π^- is within 180 $\pm$ 20 degrees were selected.

The square of the missing mass of a spectator proton was constructed for the reaction, γ + D $\rightarrow \pi^-$ + p + X and events were selected for which that value was below 1.1 GeV^2.

The background contribution from the Polychlorotrifluoroethylene (pCTFE) target cell windows and thin Aluminum cooling wires [1] was obtained from data taken with an empty target cell, scaled to the same photon flux, and analysis requirements identical to the full target data were imposed [4, 5]. The contributions to the yields from the target cell windows were thus removed by subtraction. This process was carried out independently for each of 13 $cos(\theta_\pi^{cm})$ bins and 21 W bins, ranging from 1.5 to 2.3 GeV.

B. Kinematic fitting

Kinematic fitting (KinFit) uses the constraints of energy and momentum conservation to improve the accuracy of measured quantities, and so obtain improved estimates on the momenta of undetected particles [6]. This allows a separation of reactions with additional particles in the final state, as well as reactions on bound nucleons in the target cell material, since these deviate from elementary kinematics.

In this analysis, a pre-selection of events eliminated the target cell windows with cuts on the vertex reconstruction (within the black arrows of Figure 1), leaving only the background from aluminum cooling wires to be removed by the fitting algorithm. Kinematic fitting also emphasized quasi-free reactions by significantly suppressing contributions from high-momentum neutrons in the deuteron.

For each event, a confidence level was calculated, assuming the reaction γ + (n) $\rightarrow \pi^-$ + p, where the target was assumed to have the neutron mass but unknown momentum [7]. On this confidence level distribution a requirement of $\geq$ 0.05 was applied to extract the reaction yields. This confidence level requirement was varied to investigate the impact on the extracted asymmetries (1.3 % relative) and the results of this and similar systematic studies are reflected in the first row of Table I.

C. Boosted Decision Trees

When viewing exclusive events in a quasi-4π detector such as the CLAS, many different kinematic variables can be constructed. Conventional analyses, such as discussed in (A) above, view each of these in different projections to one or two dimension and place sequential cuts on the data to extract the reaction of interest. In contrast, multivariate *Boosted Decision Trees* (BDT) can be used to view each event in a higher dimension where all cuts can be placed *simultaneously* [8, 9]. The process creates a *forest* of logical *if-else* tests for every kinematic variable and the resulting decision trees are applied to all of the available information.

In this application, π^-+p candidate events were preselected and their reconstructed vertex was required to lie within the region excluding the target cell windows (within the black arrows of Figure 1). The BDT algorithm was *trained* on the results of a Monte Carlo of the CLAS response to the reaction of interest and on the empty target data, and then used to separate each event into either *signal* or *background* [10]. This procedure retained an average of about 25% more π^- + p events than those from the method A, which resulted in smaller statistical uncertainties, and yielded asymmetry results in good agreement with the other analysis methods. Parameters of the procedure were varied to study the associated systematic uncertainties, and the results are summarized in Table I.

III. PRELIMINARY RESULTS

From an analysis of the full data set, the asymmetries resulting from the three data reduction methods are statistically consistent. As an example, E asymmetries as a function of cos θ_{π^-}, calculated in the center of mass of the γ+n system, are shown in Figure 2 for each of the three analysis methods at a sample of four different total energy bins. The magenta, red and blue points are re-

TABLE I. Estimated systematic uncertainties of E (preliminary) for each of the three analysis methods, and for beam and target polarization. (All uncertainties are relative.)

Contribution to σ_{sys}	σ_{sys}		
	BkgSub	KinFit	BDT
Analysis Parameter variation:	3.7%	3.5%	3.5%
Extrapolation to $\|\vec{p}_{miss}\|$=0:	2.2%	2.2%	2.2%
σ_{sys}(cuts):	4.3%	4.1%	4.1%
Photon beam polarization:	3.4%	3.4%	3.4%
Target polarization:	6.0%	6.0%	6.0%
σ_{sys}(polarization):	6.9%	6.9%	6.9%
σ_{sys}(total):	8.1%	8.0%	8.0%

sults from the *Background Subtraction*, *kinematic fitting* and *BDT* analyses, respectively.

A weighted average of the results from the three analyses has been used to give the best estimate of the E asymmetries. In calculating the net uncertainty, we have used standard methods to estimate the correlations between the analyses [11], which are not completely identical since the different analysis requirements result in a selection of different sets of events. The resulting asymmetries are shown in Figure 3, for a sample of twelve W bins, ranging from 1.52 to 2.28 GeV. Also plotted there are predictions from Partial Wave Analyses (PWA) by the George Washington University *SAID* group (red curves) [12] and the Bonn-Gatchina (BoGn) collaboration (black curves) [13]. The predictions are largely consistent with the asymmetry data at lower energies, but significant deviations develop with increasing energy. This is to be expected since photo-production data from the neutron are quite limited and the production amplitude is underconstrained. New PWA which include fits to these data are now underway and will undoubtedly lead to significant modifications to the neutron multipoles.

Systematic variations to the data have been studied by changing parameter values for each of the three analysis methods and the results are summarized in Table I. The systematic uncertainty associated with analysis and event processing enter the three methods in different ways, but total about 4% in each case. Nonetheless, the systematic polarization uncertainty dominates (6.9%) and leads to a total systematic uncertainty of 8% for the experiment.

This work was supported in parts by the U.S. Department of Energy, Office of Science, Office of Nuclear Physics under contract DE-AC05-06OR23177.

[1] C. D. Bass *et al.*, Nucl. Inst. Meth. Phys. Res. A **737**, 107 (2014).
[2] M. M. Lowry *et al.*, Nucl. Inst. Meth. Phys. Res. A **815**, 31 (2016).
[3] B. Mecking *et al.*, Nucl. Inst. Meth. Phys. Res. A **503**, 513 (2003).
[4] T. Kageya *et al.*, Int. J. Mod. Phys. Conf. Ser. **26**, 1460079 (2014).
[5] T. Kageya *et al.*, JPS Conf.Proc. **10**, 032009 (2016).
[6] A. G. Frodesen, O. Skjeggestad, and H. Tøfte, *Probability and Statistics in Particle Physics* (Universitetsforlaget, Bergen, Norway; ISBN 82-00-01906-3, 1979).
[7] P. Peng, *Polarization observables for single and double charged pion photo-production with polarized HD target*, Ph.D. thesis, University of Virginia (2015).
[8] H. Drucker and C. Cortes, Adv. Neural Inform. Process Sys. **8**, 479 (1995).
[9] A. Hoecker *et al.*, arXiv:physics/0703039.
[10] D. Ho, *Measurements of the E Polarization Observable for* $\gamma d \to \pi^- p(p_s)$, $\gamma d \to K^0\Lambda(p_s)$ *and* $\gamma d \to \pi^+\pi^- d(0)$ *using CLAS g14 data at Jefferson Lab*, Ph.D. thesis, Carnegie Mellon University (2015).
[11] M. Schmelling, Physics Scripta **51**, 676 (1995).
[12] R. L. Workman *et al.*, Phys. Rev C **86**, 035202 (2012).
[13] A. V. Anisovichi *et al.*, Eur. Phys J. A **48**, 15 (2012).

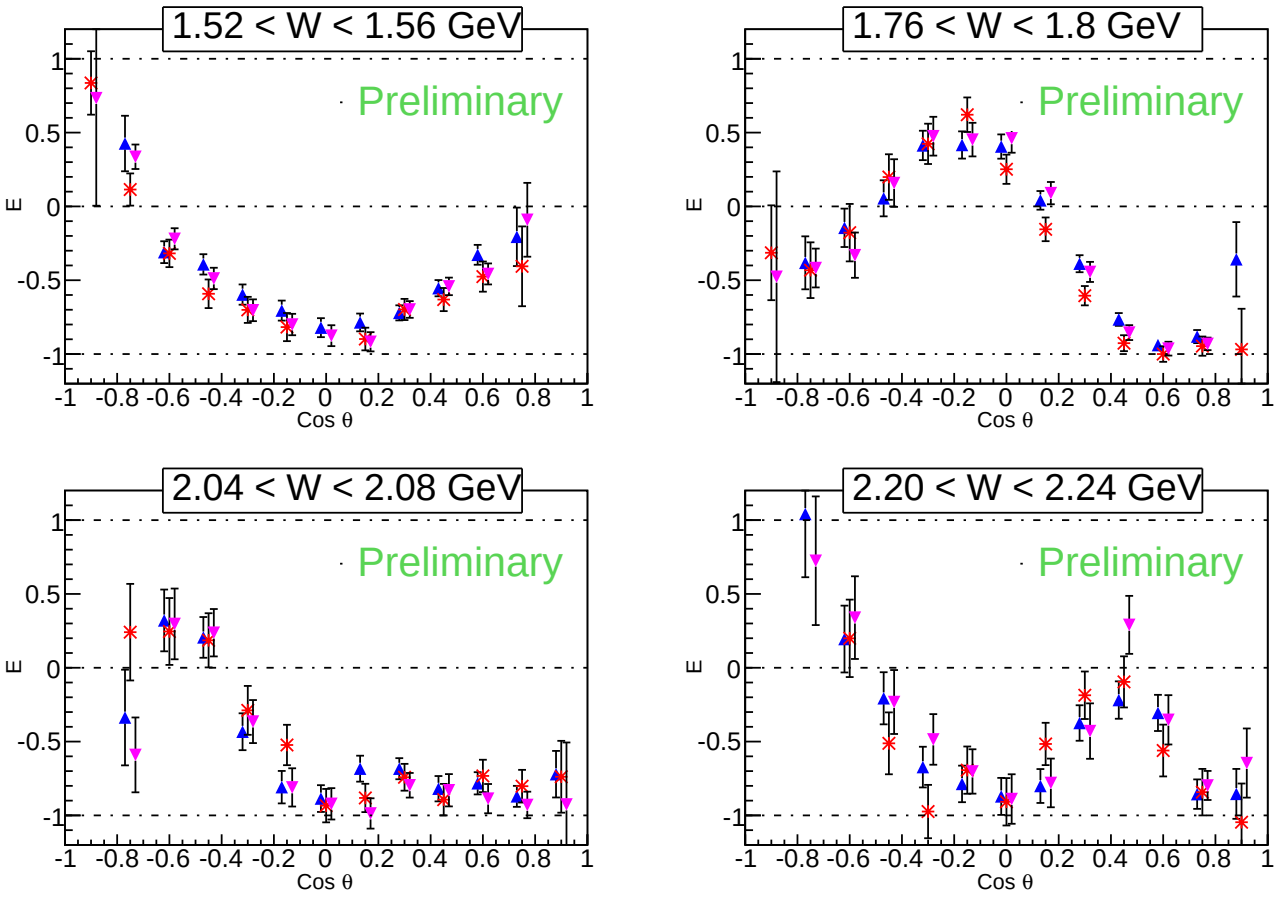

FIG. 2. Preliminary E asymmetries are plotted as a function of cos θ_{π^-} in the $\gamma+n$ CM frame from the three analysis methods (Magenta: *Background Subtraction*; Red: *kinematic fitting*; Blue: *BDT*) for (a) $1.52 \leq W \leq 1.56$ GeV, (b) $1.76 \leq W \leq 1.80$ GeV, (c) $2.04 \leq W \leq 2.08$ GeV and (d) $2.20 \leq W \leq 2.24$ GeV.

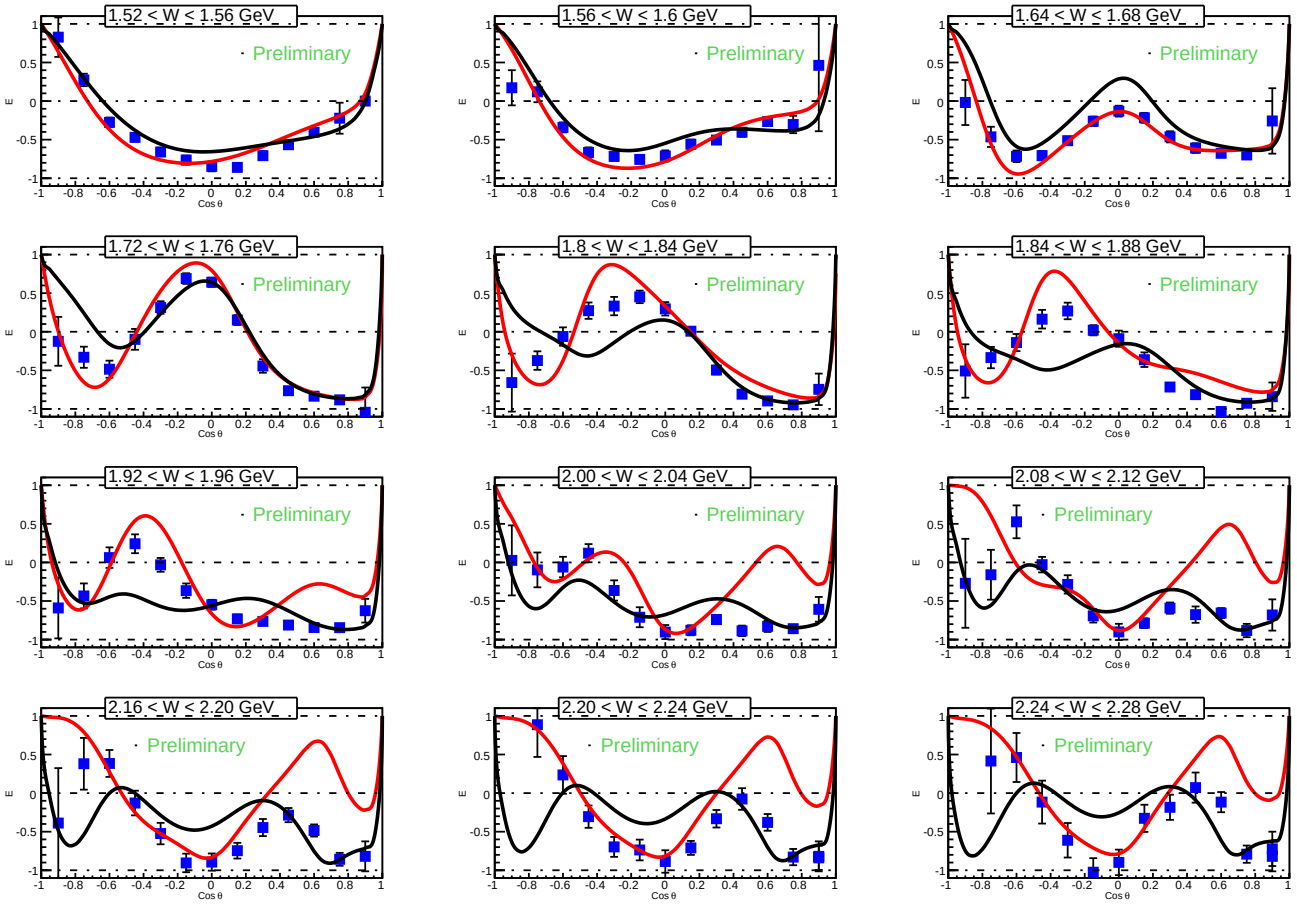

FIG. 3. Net exclusive E asymmetries, as a function of cos θ_{π^-} in the γ+n CM frame, for a sample of twelve W ranges from 1.52 to 2.28 GeV. Only statistical errors are shown. Two PWA analysis predictions are plotted for SAID[solution CM12] [12](red curves) and BoGn[solution 2011-02] [13](black curves).